The New BMW Acoustic Wind Tunnel Centre

Peter Waudby-Smith and Christopher Sooriyakumaran, Aiolos Engineering
Christoph Gabriel and Martin Grabenstein, BMW AG

Aiolos Engineering Corporation
300-135 Queens Plate Drive
Toronto, Ontario, M9W 6V1, Canada

BMW AG
D-80788 München

Peter.Waudby-Smith@aiolos.com
Christopher.Sooriyakumaran@aiolos.com
Christoph.JO.Gabriel@bmw.de

Abstract: BMW has brought into service a new dedicated acoustic wind tunnel center (AWZ) at its Research and Innovation Centre in Munich. The AWZ represents an improvement in vehicle aero-acoustic testing capabilities. The background noise level of the wind tunnel is lower than in other automotive wind tunnels, and the hemi-anechoic performance extends lower in frequency, down to 30 Hz. The aerodynamic environment, both flow stability and flow uniformity, is uncompromised, with demanding requirements met across the full wind speed range. New testing capabilities include a large frontal acoustic array with 216 microphones and a multi-location laser vibrometry system for panel vibration measurements. An interchangeable floor module section allows for different floor conditions including one with a glass floor for underbody laser vibrometry measurements, one with wheel spinners for wind-roll noise simulation, as well as one equipped with a balance for motorcycle aerodynamics. This paper will describe the wind tunnel, its acoustic and aerodynamic capabilities, the features that have enabled these capabilities to be achieved, and its measurement systems.

Contribution: 2025 FKFS Conference on Vehicle Aerodynamics and Thermal Management
15 – 16 October 2025 | Leinfelden-Echterdingen

1 Introduction

Since 1987 BMW has used a dedicated acoustic wind tunnel on Hanauerstrasse for their aero-acoustic testing (HWK). This wind tunnel was highly productive but its capabilities have been eclipsed by more modern facilities and the need for a quieter testing environment for future vehicles. In addition, the HWK is located separate from BMW's other wind tunnels, which were built after the HWK and within the BMW Research and Innovation Centre (FIZ) in Munich. In 2019 BMW selected the group comprising Habau, MCE, ETS, and Aiolos Engineering for a new acoustic wind tunnel (AWZ) and a connected testing building (WPM), with Aiolos as the technical lead for the wind tunnel. The WPM provided space for the wind tunnel control room, offices, and vehicle preparation rooms, but was otherwise separate from the wind tunnel. Design of the AWZ and WPM started at the end of 2019 and the projects were completed by the end of 2024.

The available space for the new wind tunnel was limited, leading to a vertically oriented wind tunnel. Such a vertical orientation is often used for smaller wind tunnels but never previously for such a large wind tunnel as the AWZ. Local building height restrictions led to more than half of the wind tunnel being located below ground level.

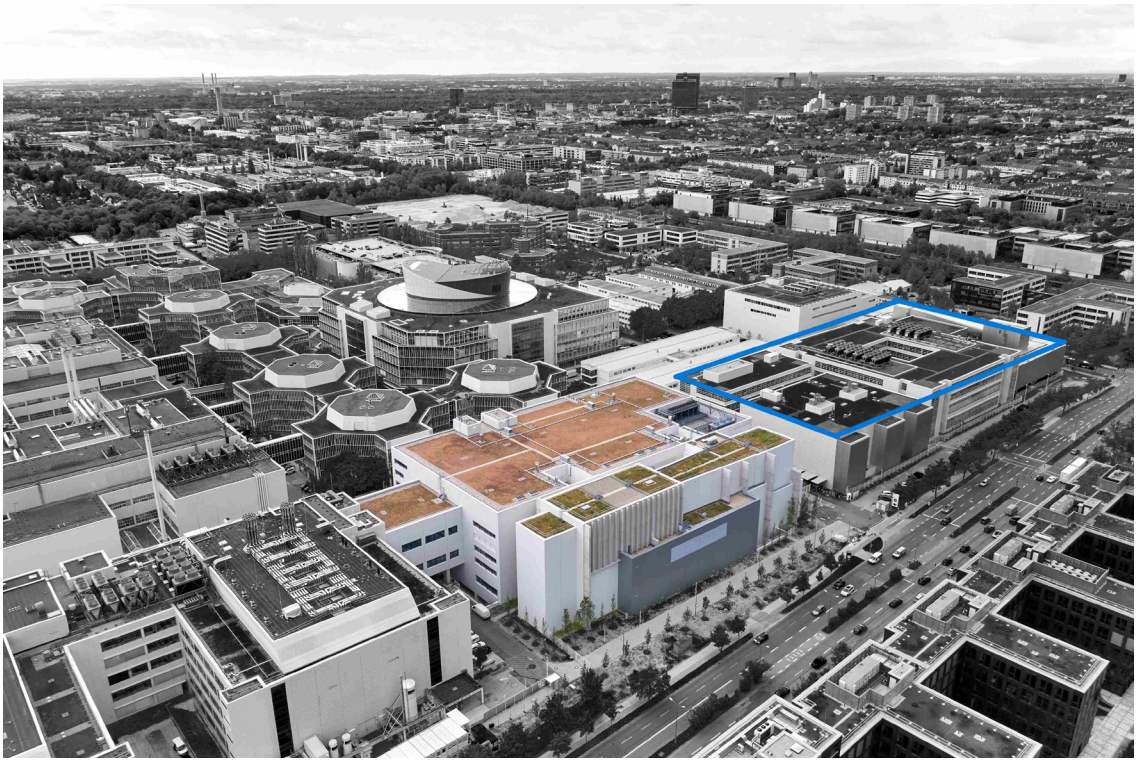

Figure 1: Aerial view of the AWZ (green roof) and WPM (red roof) beside the climatic and aerodynamic wind tunnels (blue highlight) in the BMW Research and Innovation Centre (FIZ)

Aero-acoustics is particularly important for quiet electric vehicles. With the combustion engine no longer present to mask other noise sources, primarily wind and rolling noise, these noise sources become more apparent. The AWZ is designed to address both the wind and rolling noises.

The background noise requirements represent an improvement to the performance of existing acoustic wind tunnels. The plenum cut-off frequency requirement is 30 Hz, chosen to enhance the investigation of low-frequency phenomena on the vehicle. This cut-off frequency represents a step change improvement over the 50 Hz cut-off in recent wind tunnels (e.g. [1] to [5]), requiring a new design approach for the plenum acoustic treatment. The aerodynamic performance was required to be as good as the existing aerodynamic wind tunnels at BMW [6]. The only exception was the floor boundary layer thickness – the noise contribution from a boundary layer reduction system was not considered a worthwhile compromise. In contrast, rolling noise tests, with the complex interaction between the main airflow and tire induced airflows, were required as test capabilities for the AWZ. A wheel spinner system was therefore included with one of the interchangeable floor systems. Support for this approach can be found in [7].

The test section has a nozzle size of 25 m^2. The test section incorporates a ±70° rotating 9 m diameter turntable with its centre located 6.5 m downstream of the nozzle exit plane. The turntable incorporates a unique automated removable floor mechanism to switch amongst four surfaces: A solid floor for standard aero-acoustic tests; a solid floor with four wheel spinners; a large underbody 13.2 m^2 glass floor; and a motorcycle testing unit with balance and twin wheel spinners. The turntable also includes side-mounted vehicle lifts to allow for switching of the floors without removal of the vehicle.

The test section includes a full suite of noise and vibration measurement systems, of which the fixed frontal microphone array on top of the nozzle is the most prominent.

Figure 2: Test section showing vehicle operating with wheel spinners, and frontal array above the nozzle (left) and view looking downstream with the glass floor installed and the control room window visible (right)

2 Acoustic Design Features

With its emphasis on low background noise, the circuit design includes numerous acoustic design features. Fan noise attenuation in the circuit was achieved through a combination of acoustic turning vanes, annular acoustic treatment both upstream and downstream of the fan, and extensive duct acoustic treatment. The only duct sections not treated were between corner 4 and the nozzle, and the vertical and horizontal surfaces of the fan diffuser. Surface treatments (fabric and pile fabric) were used on the airflow side of selected areas with perforated plates to minimize the self-noise from the perforated plate. These treatments were used on the collector, plenum backwall, test section diffuser, and corner 1 vanes.

A relatively high contraction ratio of 6.8:1 was chosen to reduce the flow speed in the return circuit, reduce the fan power, and enhance the test section flow quality.

Structure-borne noise issues were a significant consideration in the design of the AWZ due to the vertical orientation of the wind tunnel. For the fan itself, structural decoupling was achieved using 12 spring-mass dampers, designed to attenuate the blade passing frequency impact, located between the concrete inertial mass supporting the fan and the circuit structure.

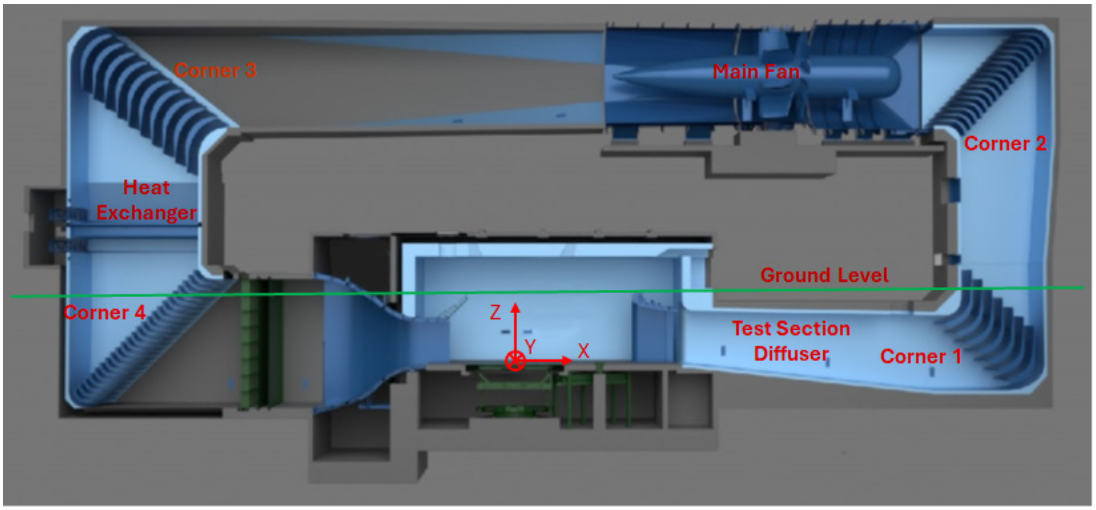

Figure 3: Layout of the AWZ Airline

The orientation of the AWZ circuit layout shown in Figure 3 is opposite to the exterior view shown in Figure 1.

2.1 Test Plenum Design

A unique feature of the AWZ is its capability for acoustic testing down to 30 Hz, achieved through the hemi-anechoic performance of the plenum. The acoustic panels of the AWZ were designed by Müller-BBM and manufactured by TAB to achieve a 30 Hz cut-off, but without the use of membrane absorbers. The depth of these panels is considerably greater than typical membrane absorber panels, but also considerably less than the 2.9 m required for a classical wedge design.

The plenum includes openings for an air exchange system, breather vents, and openings to the ceiling resonator. All of these openings feature silencers to prevent noise intrusion from outside. Flat reflective surfaces were minimized in the plenum walls and ceiling. The control room viewing window can be covered with a retractable acoustic cover.

The control of low-frequency pressure fluctuations and the axial static pressure gradient was achieved through appropriate collector and diffuser inlet sizing, and a set of four low-frequency resonators located in the circuit and above the plenum. The geometries for these components were developed in a $1/10^{th}$ scale model wind tunnel test program. The passive feedback connection developed in the model wind tunnel was not used [8].

Temperature control for the test section is set at a constant 22 °C operation regardless of the wind speed. An air exchange system is included to allow for idling of the test vehicle wind-on without requiring a closely-coupled exhaust extraction system. The air exchange system uses dry air to prevent condensation from the heat exchanger. Due to its location in the vertical cross-leg, a removeable bridge is incorporated at the heat exchanger to allow for inspection and maintenance of the heat exchanger.

3 Measurement Systems

Acoustic Measurement Systems: The wind tunnel includes a large set of acoustic measurements systems carried over from the previous HWK acoustic wind tunnel. These systems include a moveable GFaI 2.5 x 2.5 m^2 side acoustic array with 144 microphones and an interior spherical array with 48 microphones. A new fixed 4.5 m x 3 m acoustic array with 216 microphones was added to this system to allow for detailed noise investigations over the front of the test vehicle. There is provision for new side and top array units to be mounted on a large retractable open portal frame, with ceiling rails already installed and a room available behind the rear plenum wall to store the new equipment when not deployed.

Laser Vibrometry System: The wind tunnel integrates an innovative full-body laser vibrometry system. This system enables a 360° capture of vibrations on various vehicle components, setting new standards for vibro-acoustic measurement technology.

Laser Doppler Vibrometry (LDV) systems are considered the next step in vibro-acoustics as they overcome the many limitations of conventional sensors. Traditional accelerometers require glueing and wiring, which alters the investigated parameters due to mass, stiffness, and flow resistance. In contrast, LDV systems measure surface movements in a completely contactless and undistorted manner.

The system uses 10 scanning vibrometers from the Optomet SMART series, arranged to fully cover the surfaces of the vehicle. Three of these vibrometers are located below the vehicle and used with the glass floor. The other vibrometers are located on the side wall (2 each side), ceiling (2), and one behind the vehicle. All devices are synchronised via an Ethernet connection with sub-nanosecond accuracy, automatically capturing vibrations at several thousand points on the vehicle, including body, attachments, and underbody.

The measurement grid is created offline directly on the CAD model in advance to ensure efficient use of available wind tunnel time. During a test campaign, various configurations can be tested and the classic 'measure-modify-measure' cycle is reduced from days to hours. The associated software calculates phase-accurate animated 3D representations of the operational vibration modes based on reference channels such as the microphones inside the car cabin, LDVs on defined reference points, or accelerometers.

Operational modal analysis under wind load provides a precise understanding of all vibrational components involved and enables precise low-frequency measures to tackle the problem at its source rather than compensating measures such as stiff or tuned mass dampers. An example from a wind-on LDV measurement set is shown in Figure 4 below.

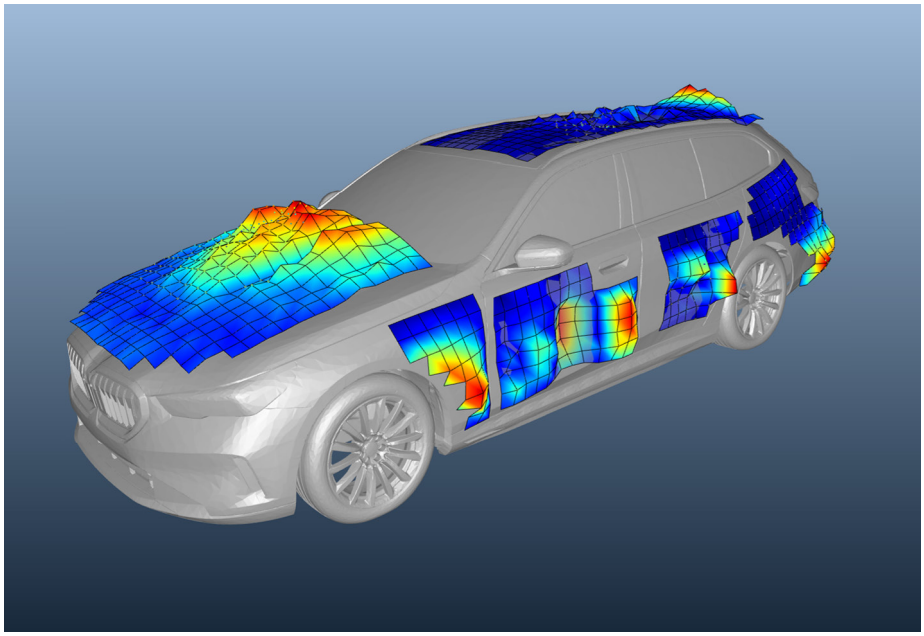

Figure 4: Example of LDV results from a BMW 5 series. The displacements shown for each section on the vehicle relate to unique frequencies relevant to that section

4 AWZ Acoustic Performance

The background noise in the AWZ was measured with a pair of GRAS 40AE freefield microphones positioned horizontally towards the turntable centre and located 6 m either side of the turntable centre at 1.2 m height. The control room window cover was in place. The overall sound pressure level (OASPL) is shown in Figure 5 and compared with published data from comparable aero-acoustic wind tunnels. The lower background noise of the AWZ is evident in this Figure. At 140 km/h the OASPL is 54.7 dB(A).

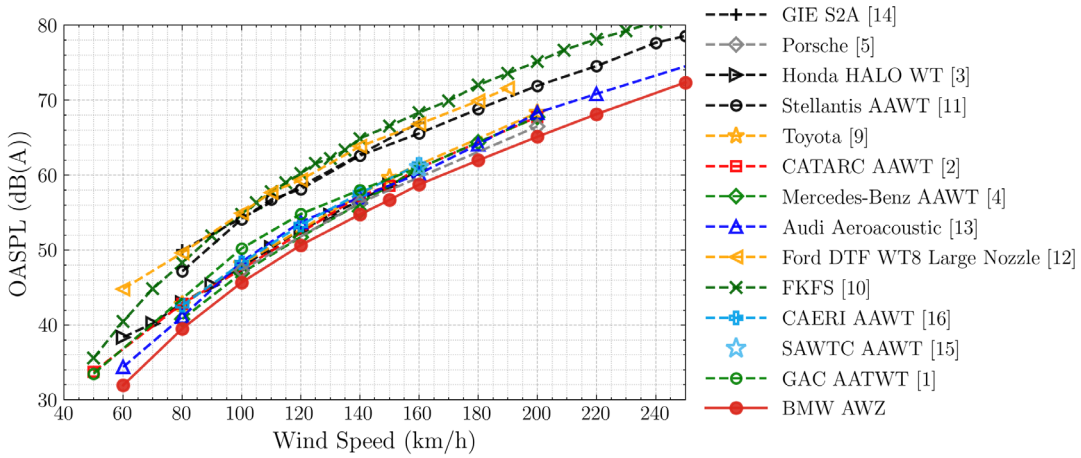

Figure 5: OASPL variation with wind speed at x, y, z = (0, 6, 1.2) m

Third-octave spectra for each wind speed are shown in Figure 6. These spectra show smoothly varying curves with increasing wind speeds without dominant noise features.

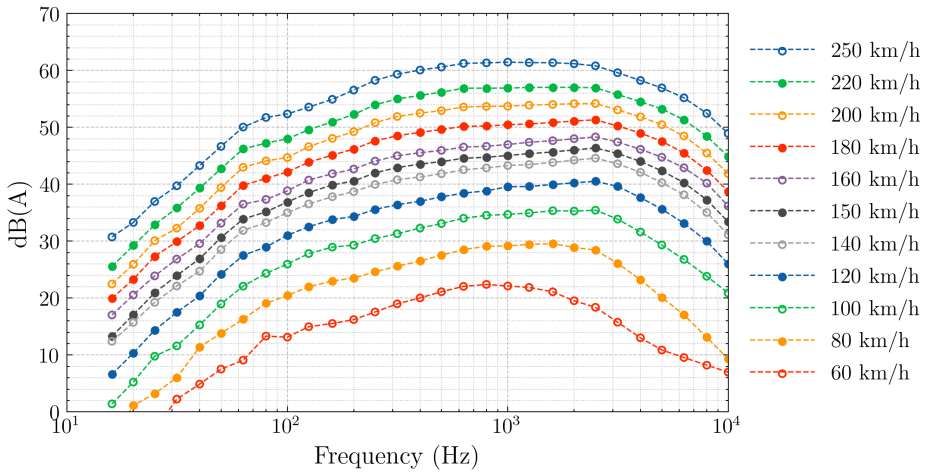

Figure 6: AWZ 1/3rd Octave Band Sound Pressure Spectra at x, y, z = (0, 6, 1.2) m

4.1 Low-Frequency Pressure Fluctuations

Low-frequency pressure fluctuation measurements were made out-of-flow 6 m either side of the turntable centreline at 0.7 m height, and in-flow at the turntable centre at a 1.2 m height. All of the measurements were made with GRAS 40AN microphones; the in-flow measurements used a GRAS RA0020 nosecone. The root-mean-square pressure fluctuations normalized by the freestream dynamic pressure are shown in Figure 7 along with data from other large automotive wind tunnels.

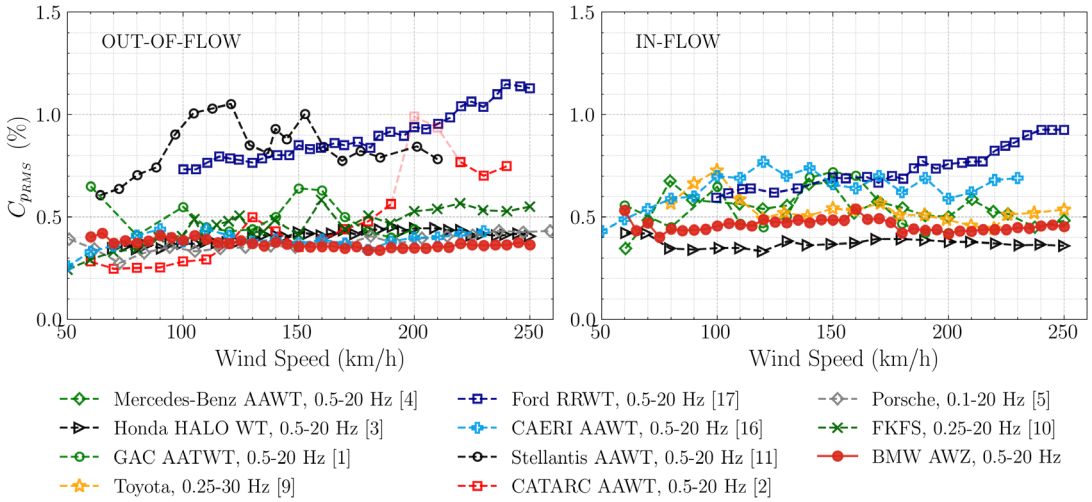

Figure 7: Out-Of-Flow (Left) and In-Flow (Right) Integrated Pressure Fluctuations

The spectral shape of the pressure fluctuations is also important. For BMW the narrowband pressure fluctuations for a frequency interval of $\Delta f = 0.1$ Hz over the range of 1-30 Hz should be less than 100 dB(Z) up to 120 km/h, and less than 105 dB(Z) up to 250 km/h. Examples of this spectral approach are shown in Figure 8 for measurements at the turntable centre axial position. Together with the Cp_{rms} data, the AWZ results show that the pressure fluctuations have been controlled and that there are no significant interactions with resonant modes of the circuit or the plenum.

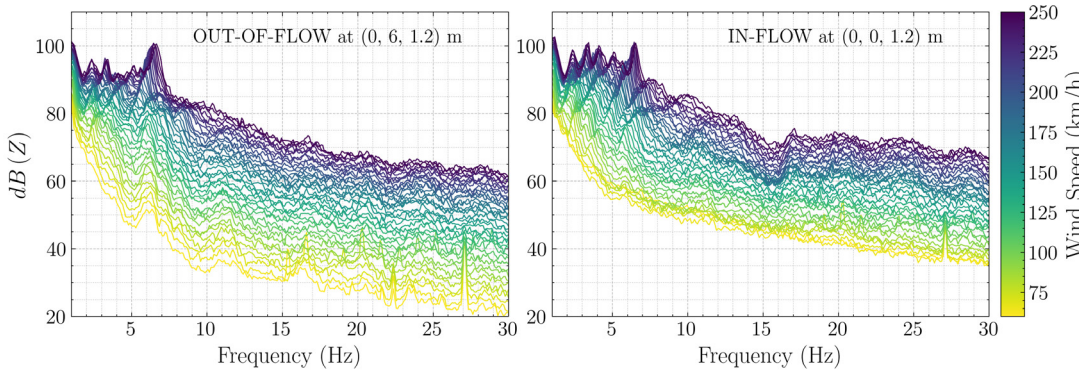

Figure 8: Narrowband low-frequency pressure fluctuation spectra, $\Delta f = 0.1$ Hz

5 Axial Static Pressure Variation

The AWZ did not include a wide-coverage in-flow traversing mechanism. A floor mounted traverser with a single pitot-static probe was used for the initial axial pressure measurements where adjustments to the collector were made. The final set of measurements were performed with a single probe mounted on a floor stand, manually moved wind-off for every 0.5 m increment. This procedure, though time-consuming, provided confidence in avoiding variable probe support interference over the length of the measurement region.

An adjustment to the static pressure variation near the nozzle exit was achieved with half-round surfaces applied to the nozzle exit, flush with the airflow surface. The half-round shape was also beneficial in terms of acoustic reflections.

Figure 9 shows the axial static pressure variation in the AWZ along with results from other wind tunnels for a similar wind speed (120 km/h to 150 km/h). The AWZ Cp variation is seen to stay within ±0.0021 over the measured range of -4.5 m to +6 m.

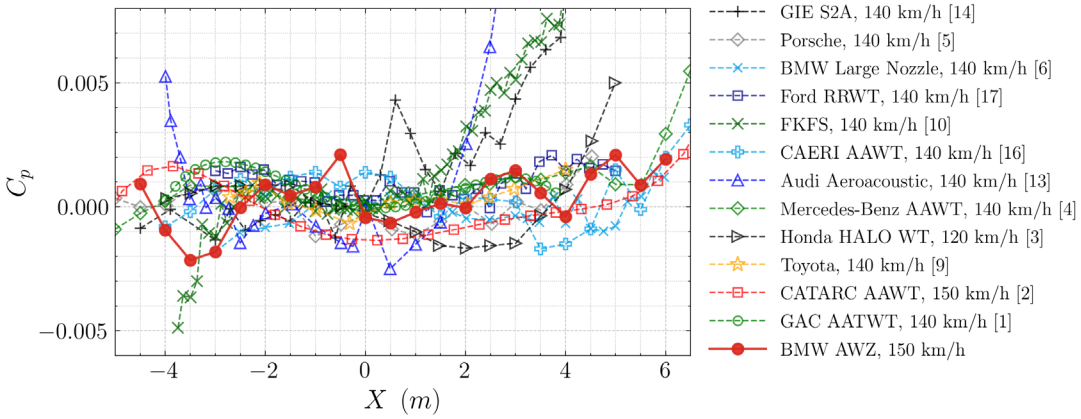

Figure 9: Axial static pressure coefficient distribution for several full-scale automotive wind tunnels. Results are relative to the turntable centre

Fourth-order curve fits were applied to the AWZ data to allow for a calculation of the pressure gradient. Plots of the resulting pressure gradient are shown in Figure 10. The pressure gradient remained within ±0.0009/m over the required axial length of -3.5 m to +5 m and for the full wind speed range of 80 km/h to 250 km/h.

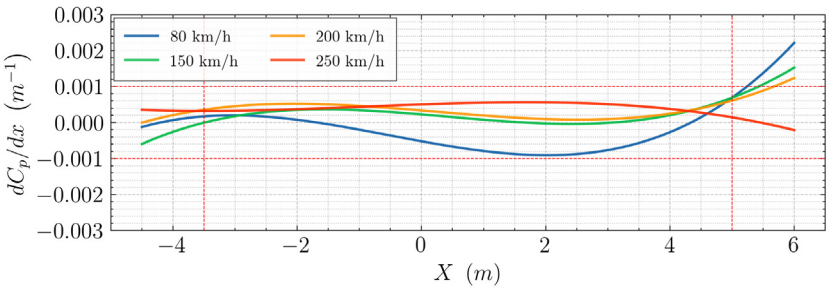

Figure 10: Axial static pressure gradient in the AWZ along Y=0 m, Z = 0.7 m

6 Flow Uniformity

The flow traversing mechanism selected for these measurements was a standalone floor-based unit with a vertical drive mechanism, shown in Figure 11. The horizontal and axial directions were manually driven. The concept, based on a traversing mechanism that was similar but with fixed probe positions on the strut [18], combined high stiffness, minimal variations in flow interference, and avoidance of fastening holes in the turntable.

Figure 11: Flow Uniformity Measurement Rig at the X = 4.5 m Test Plane

Measurements were obtained over YZ-planes extending into the jet shear layers at five discrete axial locations. Two measurement grids were used; a coarse grid with roughly 160 measurement points and a 400 mm spacing at axial locations of X = ±5.25 m, ±2.25 m, and 0 m; and an additional fine grid in the core of the jet with spacings of 200 mm at the turntable centre (X = 0). See Table 1 for further details.

The total pressure, static pressure, and flow angle uniformity measurements were made with an Aeroprobe 5+static multi-hole probe. An exposed thermally insulated 4-wire RTD sensor attached to the probe support, and a matching but fixed RTD in the flow, provided the temperature measurements (only recorded for the X = 0 m plane).

The dynamic pressure uniformity results are shown for all five planes in Figure 12. The contours use the measured dynamic pressure at each measurement location normalized by the reference freestream dynamic pressure. The progressive erosion of the uniform flow field by the shear layers is visually evident in this presentation. Although the total pressures are more uniform than the static pressure in the central region it is the erosion of the total pressure that contributes to most of the dynamic pressure fall-off in the shear layers.

Within the central region but over all five planes and all wind speeds tested the total pressure uniformity was less than 0.16% in each plane, while the static pressure uniformity was less than 0.23% (one standard deviation for both values). Further details are provided in the performance summary in Table 1.

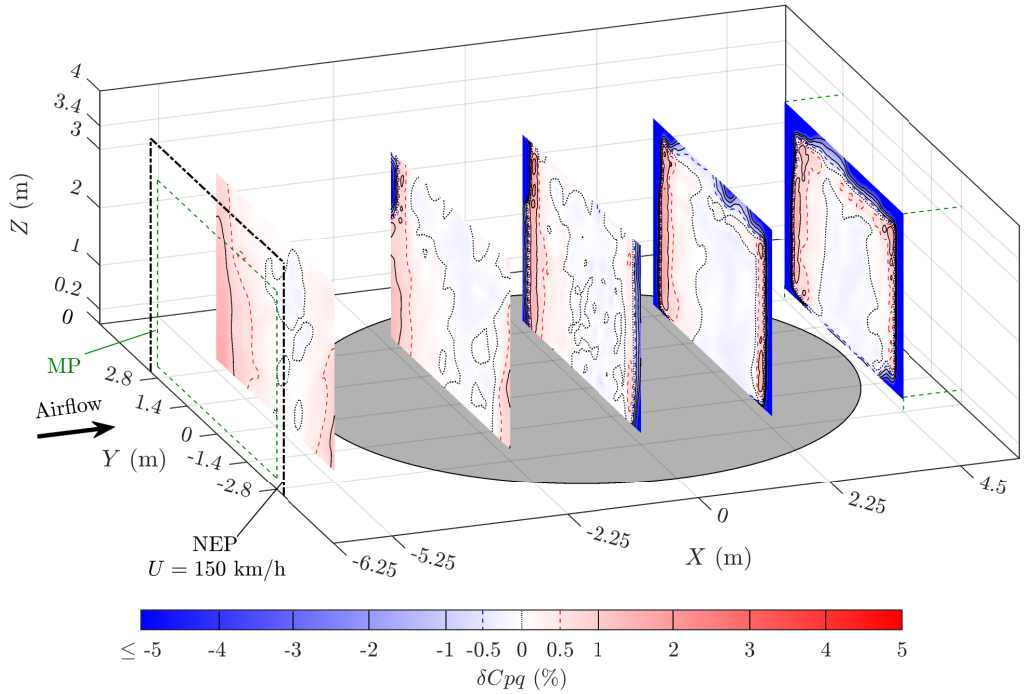

Figure 12: Dynamic Pressure Uniformity at 150 km/h
MP – Measurement Plane Boundary, NEP – Nozzle Exit Plane

The flow angle taps of the Aeroprobe probe were calibrated in-situ, with separate calibrations for each wind speed. A Leica Geosystems TS16 Total Station, located out of the flow in the plenum, was used to measure the pitch and yaw angles of the probe support for each probe position and for each wind speed at X = -5.25, 0, 4.5 m. The accuracy of these probe angle measurements was generally within ±0.02°. The flow angles are shown in a vector format in Figure 13. Within the specification planes at X =-5.25 m and 0 m the standard deviations of the flow angles were within 0.09° in pitch and 0.13° in yaw. At the X = 4.5 m plane the uniformity was only slightly degraded.

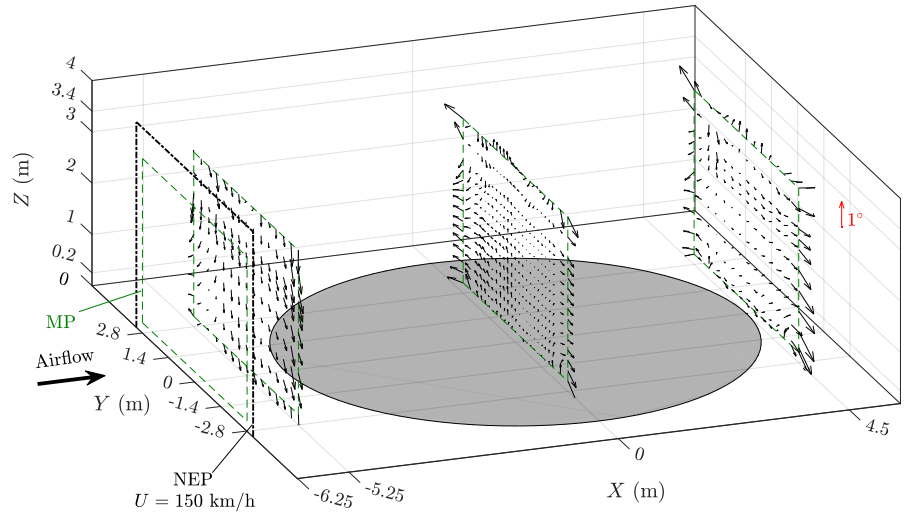

Figure 13: Flow Angle Distribution at 150 km/h

Turbulence was measured with a Dantec 55P11 single-wire hot-wire and a Dantec 54T42 miniCTA. The probe was calibrated in-situ with separate calibrations for each wind speed. The results across the full planes are shown in Figure 14. The X = 4.5 m plane could not be completed due to vibration of the probe support in the strong shear layers.

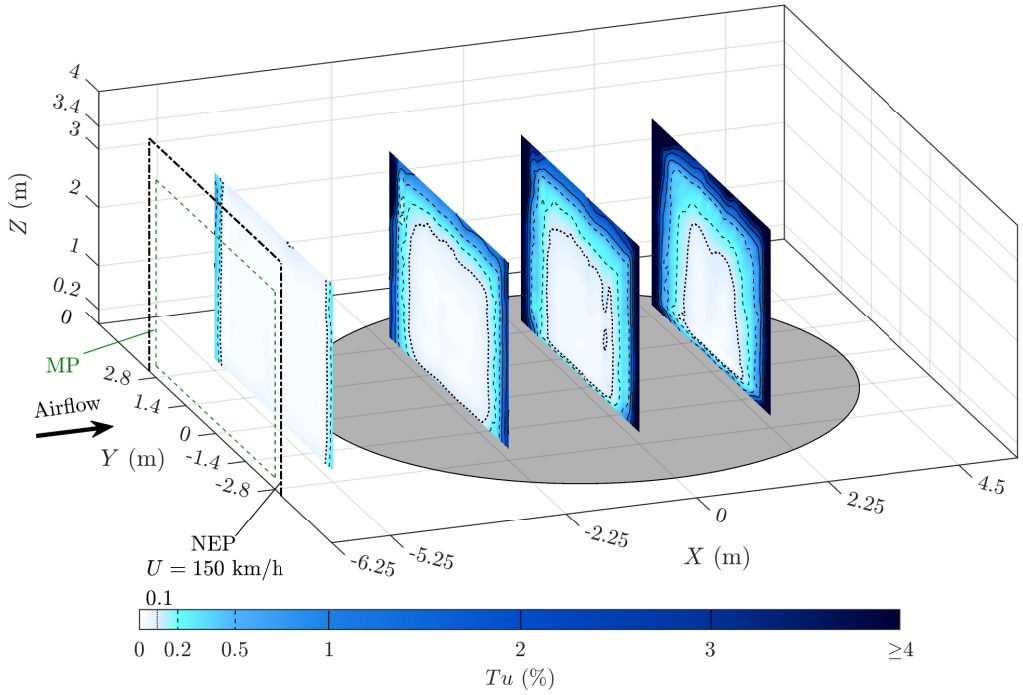

Figure 14: Turbulence intensity at 150 km/h for 10 Hz < f < 4 kHz

As is typical for an open jet, the low turbulence region is significantly eroded by the growth of the shear layers with increasing axial distance from the nozzle. The turbulence data from the four complete planes were interpolated to produce a 3-dimensional iso-contour for a single turbulence level. The iso-contour for 0.2% is shown in Figure 15. The plots show a consistent reduction in width and height with axial position for the 0.2% contour line. Also visible is the minimal but growing influence of the floor boundary layer on the turbulence. The different views of the iso-contour lines show that a typical vehicle will remain within the 0.2% turbulence lines.

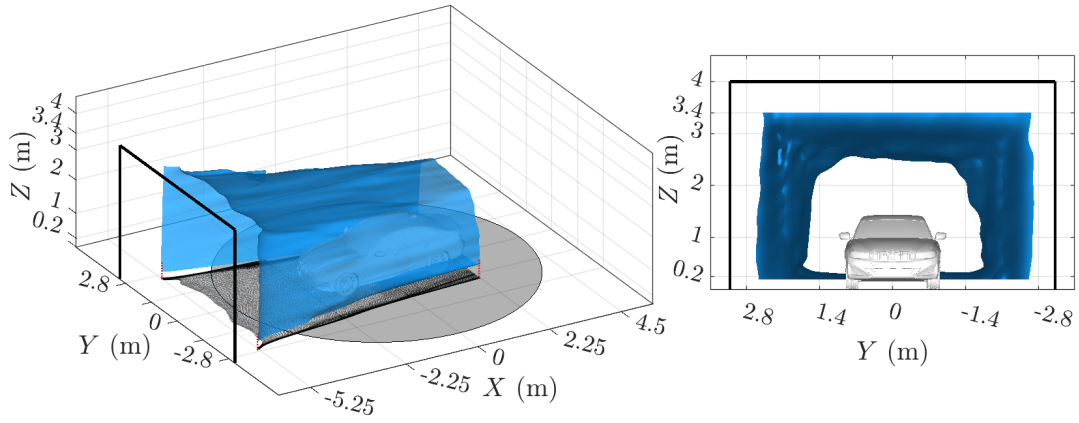

Figure 15: Iso-contour surface of Tu = 0.2% at 150 km/h

7 Summary and Conclusions

The new acoustic wind tunnel at BMW, the AWZ, brings together BMW's extensive wind tunnel testing capabilities, acoustic, aerodynamic, and climatic, into one central test centre. The AWZ represents a step improvement in the acoustic performance of automotive wind tunnels, exhibiting lower overall sound pressure levels and a lower plenum cut-off frequency. This performance was achieved while maintaining excellent flow quality. The AWZ includes a new large frontal microphone array, which when combined with the existing side and interior arrays allows for precise sound localization measurements. These acoustic systems are supplemented with a 10-camera 3D laser vibrometry system for detailed non-intrusive panel vibration measurements of the complete vehicle. Detailed underbody investigations are possible with a large glass floor. This glass floor can be switched, without removing the vehicle, to a solid floor with wheel spinners to include flow simulation at the rotating wheels. An additional floor module allows for motorcycle testing using an underfloor balance and twin wheel spinners. Taken together, the new AWZ and its testing systems expand BMW's acoustic testing capabilities to the next level within the integrated BMW research and innovation centre.

Table 1: Acoustic and Aerodynamic Performance of the AWZ

Parameter	Measurement Region	Wind Speeds	Measured Values
Background Noise OASPL	X=0, Y = ±6 m, Z = 0.7m 20 Hz - 10 kHz	60 km/h	32.0 dB(A)
		100 km/h	45.7 dB(A)
		140 km/h	54.7 dB(A)
		150 km/h	56.7 dB(A)
		200 km/h	65.1 dB(A)
		250 km/h	72.4 dB(A)
Low-frequency static pressure fluctuations, 0.5-20 Hz	X = 0, Y = ±6 m, Z=0.7m	60 – 250 km/h	$Cp_{rms} \leq 0.42\%$
	X = 0, Y = 0 m, Z=1.2 m	60 – 250 km/h	$Cp_{rms} \leq 0.55\%$
Axial static pressure variation	-3.5 m ≤ X ≤ 5 m Y = 0 m, Z = 0.7 m 4th order curve fit	80, 150, 200, 250 km/h	|Cp| ≤ 0.002 |dCp/dX| ≤ 0.0009/m
Total Pressure Uniformity	Specification Plane at X = -5.25 m, -2.25 m, 0 m, 2.25 m, 4.5 m	100/150/250 km/h	$\sigma(P_t/q) \leq$ 0.16% / 0.10% / 0.08%
Static Pressure Uniformity		100/150/250 km/h	$\sigma(P_s/q) \leq$ 0.21% / 0.22% / 0.22%
Dynamic Pressure Uniformity		100/150/250 km/h	At X = -5.25 m, $\sigma(P_q/q) \leq$ 0.21% / 0.26% / 0.24% $\sigma(P_q/q) \leq$ 0.20% elsewhere
Flow Angle Uniformity	Specification Plane at X = -5.25 m, 0 m	100/150/250 km/h	$\sigma(\alpha) \leq$ 0.09°/ 0.08°/ 0.08° $\sigma(\beta) \leq$ 0.13° / 0.12°/ 0.11°
	Specification Plane at X = 4.5 m	100/150/250 km/h	$\sigma(\alpha) \leq$ 0.11°/ 0.10°/ 0.09° $\sigma(\beta) \leq$ 0.16° / 0.15°/ 0.14°
Turbulence Intensity 10 Hz ≤ f ≤ 4 kHz	Specification Plane at X = -5.25 m	100/150/250 km/h	Tu ≤ 0.09% / 0.06% / 0.07%
Temperature Uniformity	Specification Plane at X = 0 m	100/150/250 km/h	Max,min deviation = (°C) 0.1,-0.1 / 0.1,-0.1 / 0.2,-0.5
Boundary Layer	X = -2.5 m, Y = 0 m	100/150/250 km/h	$\delta \leq$ 117 / 112 / 105 mm
Fan Power	CdA = 1.0 m^2, T = 22 °C	250 km/h	3.5 MW
Acceleration Rate	X=0, Y=0, Z = 1.2 m	0-250 km/h: 40 s; 250-20 km/hr: 30 s	
Specification Plane	|Y| ≤ 1.6 m, $z_{min} \leq Z \leq$ 2.4 m z_{min} = 0.2 m, but larger of 0.2m and 1.5δ for total pressures, 2δ for Tu		
Measurement Planes	|Y| ≤ 2.8 m, 0.2 m ≤ Z ≤ 3.4 m X = -5.25 m, -2.25 m, 0 m, 2.25 m, 4.5 m; only 100, 150 km/h		

8 Bibliography

[1] T. Bendor, V. N. Esfahani, Z. Liu, H. Yang, S. Li, X. Song, M. Liu and Z. Ma, "The Guangzhou Automotive Group Co. Aerodynamic, Acoustic, and Thermal Wind Tunnel," *SAE Technical Paper 2025-01-8878,* 2025.

[2] P. Waudby-Smith, T. Bender, C. Sooriyakumaran, Z. Yilun, H. Wang, F. Zhao, G. Fan, J. Sun and X. Liu, "The New China Automotive Technology and Research Center Aerodynamic-Acoustic and Climatic Wind Tunnels," SAE Technical Paper 2024-01-2541, 2024.

[3] S. Best, G. Bari, T. Brooker, G. Flynt, J. Walter and E. Duell, "The Honda Automotive Laboratories of Ohio Wind Tunnel," SAE Technical Paper 2023-01-0656, 2023.

[4] R. Buckisch, B. Schwartekopp and J. Pfisterer, "Daimler Aeroacoustic Wind Tunnel: 5 Years of Operational Experience and Recent Improvements," SAE Technical Paper 2018-01-5038, 2018.

[5] H. Stumpf, P. Röser, T. Wiegand, B. Pfäfflin, J. Ocker, R. Müller, W. Eckert and H.-U. Kroß, "The New Aerodynamic and Aeroacoustic wind tunnel of the Porsche AG," in 15. Internationales Stuttgarter Symposium. Proceedings. Springer Vieweg, Wiesbaden, 2015.

[6] E. Duell, A. Kharazi, S. Muller, W. Ebeling, E. Mercker, "The BMW AVZ Wind Tunnel Center", SAE Technical Paper 2010-01-0118, 2010.

[7] E. Rajaratnam and D. Walker, " Experimental and Computational Study of the Flow around a Stationary and Rotating Isolated Wheel and the Influence of a Moving Ground Plane", 2019-01-0647, 2019.

[8] P. Waudby-Smith, A. Joshi, C. Sooriyakumaran, C. Gabriel, M. Grabenstein, “Using a Passive Feedback Connection to Control Low-Frequency Pressure Fluctuations in a Wind Tunnel,” Canadian Acoustics 50, no. 1 (2022): 11-17.

[9] K. Tadakuma, T. Sugiyama and K. Maeda, "Development of Full-Scale Wind Tunnel for Enhancement of Vehicle Aerodynamic and Aero-Acoustic Performance," SAE Technical Paper 2014-01-0598, 2014.

[10] R. Blumrich, N. Widdecke, J. Wiedemann, A. Michelbach, F. Wittmeier and O. Beland, "New FKFS Technology at the Full-Scale Aeroacoustic Wind Tunnel of University of Stuttgart," SAE Int. J. Passeng. Cars - Mech. Syst., vol. 8, no. 1, pp. 294-305, 2015.

[11] J. Walter, E. Duell, B. Martindale, S. Arnette, R. Geierman, M. Gleason and G. Romberg, "The DaimlerChrysler Full-Scale Aeroacoustic Wind Tunnel," SAE Technical Paper 2003-01-0252, 2002.

[12] J. Walter, E. Duell, B. Martindale, S. Arnette, P. Nagle, W. Gulker, S. Wallis and J. Williams, "The Driveability Test Facility Wind Tunnel No. 8," SAE Technical Paper 2002-01-0252, 2002.

[13] G. Wickern and N. Lindener, "The Audi Aeroacoustic Wind Tunnel: Final Design and First Operational Experience," SAE Technical Paper 2000-01-0868, 2000.

[14] P. Waudby-Smith, T. Bender and R. Vigneron, "The GIE S2A Full-Scale Aero-acoustic Wind Tunnel," SAE Technical Paper 2004-01-0808, 2004.

[15] He, Y., Yang, Z., and Wang, Y., “Wind Noise Testing at the Full Scale Aeroacoustic Wind Tunnel of Shanghai Automotive Wind Tunnel Center,” In: Bargende, M., Wiedemann, H.C., Reuss, J. (eds.), 14. Internationales Stuttgarter Symposium. Proceedings, Springer Fachmedien, Wiesbaden, 2014.

[16] L. Xu, X. Zhu, Q. Wang, et.al., “The New China Automotive Engineering Research Institute co., Ltd Full-Scale Aero-Acoustic Wind Tunnel”, SAE Technical Paper 2025-01-8779, 2025.

[17] P. Nagle, T. Brooker, G. Bari, J. Toth, et al., “The Ford Rolling Road Wind Tunnel,” SAE Technical Paper 2023-1-0654 (2023).

[18] E. Ljungskog, S. Sebben, and A. Broniewicz, "Uncertainty Quantification of Flow Uniformity Measurements in a Slotted Wall Wind Tunnel", SAE Technical Paper 2019-01-0656, 2019.